Evolution of the critical pressure with increasing Fe substitution in the heavy fermion system $URu_{2-x}Fe_xSi_2$

C. T. Wolowiec,[1,2] N. Kanchanavatee,[1,2] K. Huang,[2,3] S. Ran,[1,2] and M. B. Maple[1,2,3,*]

[1] *Department of Physics, University of California, San Diego, La Jolla, California 92093, USA*
[2] *Center for Advanced Nanoscience, University of California, San Diego, La Jolla, California 92093, USA*
[3] *Materials Science and Engineering Program, University of California, San Diego, La Jolla, California 92093, USA*

(Dated: August 1, 2016)

Measurements of electrical resistivity, $\rho(T)$, were performed under quasi-hydrostatic pressure up to $P \sim 2.2$ GPa to determine the pressure dependence of the so called "hidden order" (HO) and large-moment antiferromagnetic (LMAFM) phases for the $URu_{2-x}Fe_xSi_2$ system with $x = 0.025$, 0.05, 0.10, 0.15, and 0.20. As the Fe concentration (x) is increased, we observed that a smaller amount of external pressure, P_c, is required to induce the HO $\rightarrow$ LMAFM phase transition. A critical pressure of $P_c \sim 1.2$ GPa at $x = 0.025$ reduces to $P_c \sim 0$ at $x = 0.15$, suggesting the $URu_{2-x}Fe_xSi_2$ system is fully expressed in the LMAFM phase for $x \geq x_c^* = 0.15$, where x_c^* denotes the ambient pressure critical concentration of Fe. Using a bulk modulus calculation to convert x to chemical pressure, $P_{ch}(x)$, we consistently found that the induced HO $\rightarrow$ LMAFM phase transition occurred at various combinations of x_c and P_c such that $P_{ch}(x_c) + P_c \approx 1.5$ GPa, where x_c denotes those critical concentrations of Fe that induce the HO $\rightarrow$ LMAFM phase transition for the $URu_{2-x}Fe_xSi_2$ compounds under pressure. We performed exponential fits of $\rho(T)$ in the HO and LMAFM phases in order to determine the pressure dependence of the energy gap, Δ, that opens over part of the Fermi surface in the transition from the paramagnetic (PM) phase to the HO/LMAFM phase at the transition temperature, T_0. The change in the pressure variation of $\Delta(P)$ at the HO $\rightarrow$ LMAFM phase transition is consistent with the values of P_c determined from the $T_0(P)$ phase lines at the PM $\rightarrow$ HO/LMAFM transition.

PACS numbers: 71.27.+a, 72.10.Di, 74.62.Dh, 74.62.Fj

I. INTRODUCTION

Subsequent to the initial bulk property measurements that were performed on the heavy fermion superconductor URu_2Si_2 in the mid 1980s,[1–3] researchers have yet to identify the order parameter (OP) associated with the so called "hidden order" (HO) phase observed at the transition temperature $T_0 \approx 17.5$ K. In the bulk, the key signatures of the second-order symmetry-breaking transition are (1) the anomalous upturn in the electrical resistivity, $\rho(T)$, that is reminiscent of a spin density wave (SDW) feature as observed, for instance, in the $\rho(T)$ data for elemental chromium near $T_N = 311$ K,[4] and (2) the large Bardeen-Cooper-Schrieffer (BCS)-like feature observed in the specific heat, $C(T)$, below $T_0 = 17.5$ K. From the specific heat anomaly, it was originally determined that a considerable amount of entropy, $\Delta S \approx 0.2R\ln(2)$, is released during the transition.[1,2] From the exponential temperature dependence of the specific heat and the reduction of the electronic contribution to the specific heat,[2] γT, a partial gapping scenario was proposed in which an energy gap, $\Delta \approx 130$ K,[1,2] is attributed to a charge- or spin- density wave (CDW or SDW) that forms over ∼40 % of the Fermi surface with the remainder of the Fermi surface gapped by the superconductivity that occurs below $T_c \approx 1.5$ K.[2,5] For the past three decades, the intense search for the OP in the HO phase has been accompanied by a large effort to explain the reduction in entropy that occurs during the transition to the HO phase as well as to determine the origin of the energy gap, Δ, near the transition temperature T_0. For a comprehensive survey of the experimental and theoretical research regarding the URu_2Si_2 compound, the reader is referred to Refs. 6 and 7.

Research at ambient pressure on the URu_2Si_2 compound reveals the existence of a second-order phase transition from a highly correlated paramagnetic (PM) phase above T_0 to the HO phase below T_0 that exhibits antiferromagnetic (AFM) order with a very small ordered moment of $\mu \sim (0.03 \pm 0.02)\mu_B$ per U atom that is aligned parallel to the c axis (in the simple tetragonal structure).[8,9] It is interesting to note that this small value for the magnetic moment in the HO phase is two orders of magnitude smaller than values for the magnetic moment of $\mu \sim 1.6 - 2.9\mu_B$ per U atom observed in other magnetically ordered compounds from the UT_2Si_2 series where T is a d-electron transition element.[10,11] This uniquely tiny magnetic moment observed in the HO phase in URu_2Si_2 is too small to account for the loss of entropy, ΔS, during the PM $\rightarrow$ HO transition. It is now believed that the small moment antiferromagnetic (AFM) order is not intrinsic to the HO phase but rather due to the existence of small pockets of the high pressure large-moment antiferromagnetic (LMAFM) phase that are stabilized by the extrinsic strain that can occur in preparing the sample for measurement.[12,13] This small concentration of the LMAFM phase can produce an average moment of a few one-hundreths of a Bohr magneton (μ_B) per U atom. An extensive amount of pressure research on HO in URu_2Si_2 reveals, in addition

* Corresponding Author: mbmaple@ucsd.edu

TABLE I. Values of the critical pressure, P_c, and the pressure dependence ($\partial T_{HO}/\partial P$) in the HO phase along with the type of measurement for the URu_2Si_2 ($x = 0$) parent compound from previous reports.

Year	Reference	Critical Pressure (GPa)	$\partial T_{HO}/\partial P$ (K GPa^{-1})	Measurement type
1987	McElfresh[16]	$P_c > 1.3$	1.3 ± 0.1	$\rho(T)$
1999	Amitsuka[14]	$P_c = 1.5$	1.3 ± 0.1	elastic NS
2001	Matsuda[15]	$P_c = 1.5$	–	^{29}Si NMR
2003	Motoyama[17]	$P_c = 1.1$ - 1.5	1.0 ± 0.1	dilatometry
2004	Amato[18]	$P_c \sim 1.4$	–	μSR
2007	Jeffries[19]	$P_c = 1.5$	1.0 ± 0.1	$\rho(T)$
2008	Hassinger[20]	$P_c \sim 1.3$	1.1 ± 0.1	$\rho(T)$
2010	Butch[21]	$1.3 > P_c > 1.5$	1.3 ± 0.1	elastic NS, $\rho(T)$

to the second-order PM → HO transition, the existence of a first-order (symmetry-breaking) transition from the small moment HO phase to the LMAFM phase which has a larger magnetic moment of $\mu \sim 0.4\mu_B$ per U atom that is also aligned parallel to the c axis.[12–15] The first-order transition into the high pressure LMAFM phase is observed to occur at critical pressures that range from $P_c \approx 0.5$ GPa (as $T \to 0$) to $P_c \approx 1.5$ GPa (for $T = T_0$). Table I provides a sampling of the variety of pressure research which includes measurements of electrical resistivity ($\rho(T)$),[16,19–21] elastic neutron scattering (NS),[14,21] thermal expansion (dilatometry),[17] muon spin resonance (μSR),[18] and nuclear magnetic resonance (^{29}Si NMR).[15] Together, the previous reports seem to indicate that $P_c \sim 1.5$ GPa is perhaps an upper bound value on the applied critical pressure that induces the first-order phase transition from the HO phase to the LMAFM phase.

Recent results from a number of ambient pressure experiments reveal that by tuning either polycrystalline[22] or single crystal[23,24] samples of URu_2Si_2 with the isoelectronic substitution of Fe for Ru, it is possible to reach the same high pressure LMAFM phase in which the first-order HO → LMAFM phase transition at ambient pressure now occurs at some critical value of Fe concentration, $x_c^* \approx 0.1 - 0.2$. Furthermore, there is a remarkable correspondence observed in the evolution of T_0 with increasing Fe concentration for the range $x = 0$ to 0.3, when compared with the results of experiments in which URu_2Si_2 is tuned with increasing applied pressure, P.[19] It has been suggested that the similarities between the T_0 vs. x and T_0 vs. P phase boundaries are a consequence of the effective reduction in the volume of the unit cell in which the substitution of the smaller Fe ions for Ru acts as a "chemical pressure", P_{ch}, that tracks well with the effects of applied pressure, P.[22–24]

In the research reported herein, we simultaneously tuned the URu_2Si_2 compound with both Fe substitution, x, and applied external pressure, P, in an effort to further explore the suggestion, as made initially in Ref. 22, that there is an equivalence between the application of pressure, P, and chemical pressure, $P_{ch}(x)$, in inducing the HO → LMAFM phase transition. We found that we could bias the parent compound with "chemical pressure" toward the LMAFM phase by systematically introducing small levels of Fe into the URu_2Si_2 compound, such that a smaller amount of applied external pressure is required to induce the transition to the high pressure LMAFM phase. Remarkably, we observed the consistent manner in which chemical pressure, $P_{ch}(x)$, and applied pressure, P, are "additive" such that $P_{ch}(x_c) + P_c \approxeq 1.5$ GPa at the first-order HO → LMAFM phase transition. (Herein, the symbol x_c is used to denote those "critical" concentrations of Fe that induce the HO → LMAFM phase transition in $URu_{2-x}Fe_xSi_2$ compounds under pressure.) Hence, the predictability in which $P_{ch}(x_c)$ and applied critical pressure P_c combine to induce the HO → LMAFM phase transition can serve as a guide for future research on the $URu_{2-x}Fe_xSi_2$ system under pressure. We also note that tuning the URu_2Si_2 compound simultaneously with both x and P may serve as a workaround to some of the limitations encountered in pressure experiments so that larger regions of phase space might be studied. To this point, we were able to track the suppression of the critical pressure, P_c, and hence the tricritical point, ($T_0(P_c)$, P_c), in the T_0 vs. P phase diagram, as a function of Fe concentration, x, for the five $URu_{2-x}Fe_xSi_2$ ($x = 0.025$, 0.05, 0.10, 0.15, and 0.20) compounds.

The T_0 vs. P phase diagrams presented in this work are based on measurements of electrical resistivity, $\rho(T)$, under quasi-hydrostatic pressure up to $P = 2.2$ GPa for the five $URu_{2-x}Fe_xSi_2$ ($x = 0.025$, 0.05, 0.10, 0.15, and 0.20) compounds. Additionally, we employed a theoretical model of electrical resistivity[25] which we were able to fit to the $\rho(T)$ data for $T < T_0$ in order to extract values of the charge energy gap, Δ, as a function of pressure, P. The changes observed in the pressure dependence of the charge energy gap, $\Delta(P)$, are consistent with the values of the critical pressure P_c that were determined from the T_0 vs. P phase diagrams.

II. EXPERIMENTAL DETAILS

Single crystals of $URu_{2-x}Fe_xSi_2$ were grown according to the Czochralski method in a Techno Search TCA 4-5 Tetra-Arc furnace under a zirconium-gettered argon atmosphere. The quality of the single crystal samples were determined by Laue X-ray diffraction patterns performed with a Photonic Science PXS11 X-ray measurement system together with X-ray powder diffraction (XRD) measurements performed with a Bruker D8 Discover X-ray diffractometer that uses Cu-K α radiation. The XRD patterns were fitted via the Rietveld refinement technique using the GSAS + EXPGUI software package.

Annealed Pt wire leads were affixed with silver epoxy to gold-sputtered contact surfaces on each sample in a standard four-wire configuration. The single crystal samples were cleaved along the basal plane of the tetragonal structure of the sample and the measurements of $\rho(T)$ were made with current running parallel to the a

axis. The orientation of the single-crystal samples of $URu_{2-x}Fe_xSi_2$ were confirmed from Laue X-ray diffraction patterns.

Electrical resistivity $\rho(T)$ measurements were performed on single crystals of $URu_{2-x}Fe_xSi_2$ under applied pressure up to $P = 2.2$ GPa for Fe concentrations $x = 0.025$, 0.05, 0.10, 0.15, and 0.2. A 1:1 mixture by volume of n-pentane and isoamyl alcohol was used to provide a quasi-hydrostatic pressure transmitting medium and the pressure was locked in with the use of a beryllium copper clamped piston-cylinder pressure cell. The pressure dependence of the superconducting transition temperature, T_c, of high purity Sn was used as a manometer. The superconducting transition of the Sn manometer was measured inductively and the pressure dependence of T_c was calibrated against data from Ref. 26. Measurements of $\rho(T)$ were performed upon warming from ~ 1 to 300 K in a pumped ^{4}He dewar and the temperature was determined from the four-wire resistivity of a calibrated Cernox sensor which was thermally sunk to the beryllium copper pressure clamp. For the $URu_{2-x}Fe_xSi_2$ compounds with $x = 0.05$ and 0.15, a second set of $\rho(T)$ measurements were performed in reverse by releasing pressure from the pressurized cell from 2.2 GPa down to atmospheric pressure.

III. RESULTS AND DISCUSSION

Enhancement of T_0 with Fe substitution

The effect of Fe substitution on the PM $\rightarrow$ HO/LMAFM transition temperature, T_0, in the $URu_{2-x}Fe_xSi_2$ system for $x = 0.025$, 0.05, 0.10, 0.15, and 0.20 was determined from measurements of $\rho(T)$ at ambient pressure. The temperature dependence of the electrical resistivity, $\rho(T)$, in the vicinity of T_0 for the five compounds $URu_{2-x}Fe_xSi_2$ ($x = 0.025$, 0.05, 0.10, 0.15, and 0.20) is shown in the inset of Fig. 1. The PM $\rightarrow$ HO/LMAFM transition temperature, T_0, is defined in this report as the temperature at which there is a minimum in $\rho(T)$ (which occurs just prior to cooling through the small upturn in $\rho(T)$) as indicated by the black arrows shown in the inset of Fig. 1. (In this report, we denote the PM $\rightarrow$ HO transition temperature as T_{HO}, the PM $\rightarrow$ LMAFM transition temperature as T_N, and traditionally reserve the use of T_0 to refer to T_{HO} and T_N, collectively.) The enhancement of T_0 with increasing Fe concentration is apparent from the shift of the minimum in $\rho(T)$ to higher temperatures such that for $x = 0.025$, 0.05, 0.10, 0.15, and 0.20, the values of T_0 are 16.6, 17.0, 17.7, 18.1, and 21.4 K, respectively. The values of T_0 at ambient pressure for the compounds $URu_{2-x}Fe_xSi_2$ ($x = 0$, 0.025, 0.05, 0.10, 0.15, and 0.20) are represented by the six symbols in color that are superimposed on the T_0 vs. x phase diagram as displayed in Fig. 1. (The single data point in green at $T = 16.5$ K, which corresponds to the URu_2Si_2 ($x = 0$) compound, was taken from Ref. 19.)

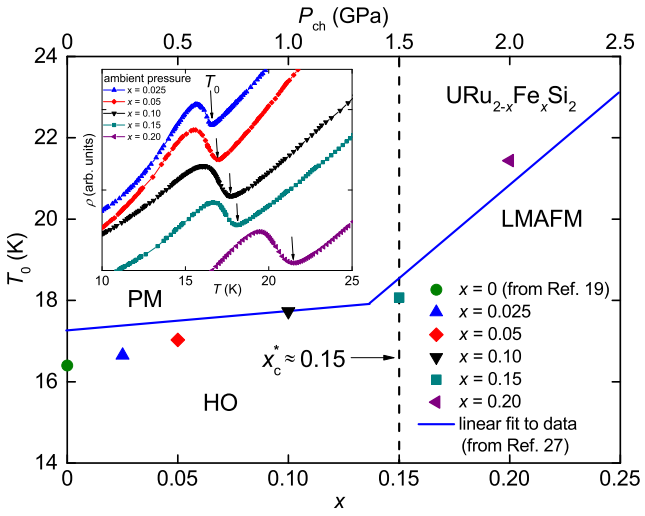

FIG. 1. (Color online) The T_0 vs. x phase diagram at ambient pressure constructed from measurements of $\rho(T)$ for the $URu_{2-x}Fe_xSi_2$ system. The two sloped solid-blue lines which intersect near the critical concentration at $x_c^* = 0.15$ represent the $T_0(P)$ boundary line between the PM phase and the HO/ LMAFM phase and are linear fits to the T_0 vs. x data taken from Ref. 27 (see text). The six symbols in color superimposed on the T_0 vs. x phase diagram are the ambient pressure values of T_0 (see inset) determined from measurements of $\rho(T)$ under pressure for the single crystal samples of $URu_{2-x}Fe_xSi_2$ with $x = 0$, 0.025, 0.05, 0.10, 0.15, and 0.20. (The green data point shown at $x = 0$ was taken from a previous study of the URu_2Si_2 parent compound under pressure.[19]) The values of x in the lower x-axis have been converted to values of "chemical pressure" $P_{ch}(x)$ which appear in the upper x-axis. Inset: Measurements of electrical resistivity, $\rho(T)$, at ambient pressure in the vicinity of the HO/LMAFM transition for the $URu_{2-x}Fe_xSi_2$ ($x = 0.025$, 0.05, 0.10, 0.15, and 0.20) compounds. The curves have been shifted vertically for clarity in illustrating the evolution of T_0 with increasing x. The HO/LMAFM transition temperature, T_0, is defined as the temperature at which there is a minimum in $\rho(T)$ as indicated by the black arrows.

From the T_0 vs. x phase diagram, the evolution of T_0 is shown to increase with Fe concentration, x, at a constant rate up until $x \approx 0.15$ at which point the rate of increase in T_0 with x abruptly increases. The two solid-blue lines, which meet near the critical concentration at $x_c^* = 0.15$, represent the $T_0(x)$ boundary line between the PM phase and the HO/ LMAFM phase and are linear fits to the T_0 vs. x data taken from Ref. 27. The observed "kink" in the $T_0(x)$ data near $x_c^* = 0.15$ marks the point at which the compound undergoes a first-order phase transition from the HO phase to the LMAFM phase at ambient pressure. The critical value of Fe concentration, $x_c^* = 0.15$, was determined in this report to be the smallest concentration of Fe in the $URu_{2-x}Fe_xSi_2$ system at ambient pressure for which there is a (nearly) homogenous manifestation of the LMAFM phase throughout the sample. Here, we use the symbol x_c^* to denote the ambient pressure critical concentration of Fe to distinguish it from the symbol x_c,

which will be reserved for those "critical" concentrations of Fe that induce the HO → LMAFM phase transition in $URu_{2-x}Fe_xSi_2$ compounds under pressure. Our determination of $x_c^* = 0.15$ is directly based on measurements of $\rho(T)$ for the $URu_{2-x}Fe_xSi_2$ (x = 0.025, 0.05, 0.10, 0.15, and 0.20) system under pressure and will be revisited later in our discussion regarding the effect of pressure on the HO → LMAFM phase transition for the $URu_{2-x}Fe_xSi_2$ series with $x = 0.025$, 0.05, 0.10, 0.15, and 0.20.

For now, we note that bulk property measurements of electrical resistivity (and also specific heat) performed on the URu_2Si_2 ($x = 0$) parent compound under applied pressure, P, or on the Fe-substituted compounds $URu_{2-x}Fe_xSi_2$ that are tuned with x, do not easily distinguish between the HO and LMAFM phases. The value of the critical concentration, $x_c^* = 0.15$, reported herein as the location of the "kink" in the T_0 vs. x phase diagram that marks the first-order phase transition from the HO phase to the LMAFM phase is consistent with values reported for the critical concentration that were determined from other types of measurements. Magnetic neutron diffraction experiments performed on the $URu_{2-x}Fe_xSi_2$ system for $x \leq 0.7$ reveal an abrupt increase in the uranium magnetic moment at $x = 0.1$.[23] A notable "kink" in the T_0 vs. x phase diagram at $x \approx 0.15$ was determined from both the magnetic neutron diffraction experiments and also measurements of specific heat.[23] Optical conductivity experiments performed on the $URu_{2-x}Fe_xSi_2$ system for x = 0, 0.05, 0.10 and 0.3 reveal that at $x = 0.10$ and below $T_0 = 18.5$ K, the compound may exist as a mixture of the HO and LMAFM phases suggesting that a full manifestation of the LMAFM phase occurs for some level of Fe concentration $x > 0.10$.[24]

The reduction in the unit cell volume associated with the substitution of smaller isoelectronic Fe ions for Ru ions in URu_2Si_2 can be interpreted as the result of "chemical pressure", P_{ch}, which can be determined from a conversion of x to $P_{ch}(x)$.[22] The chemical pressure, $P_{ch}(x)$, was determined from a calculation using the isothermal compressibility, κ_T, which, in general, relates the reduction in the volume, V, to the pressure, P, that is applied to a material. In the present context, the "chemical pressure", $P_{ch}(x)$, is determined from the linear decrease in the unit cell volume, V, that occurs with increasing levels of Fe concentration, x. The Fe concentration, x, that appears in the lower x-axis of Fig. 1 has been converted to $P_{ch}(x)$, which is displayed in the upper x-axis of the same figure. The conversion of x to $P_{ch}(x)$ is discussed in more detail below and will facilitate the discussion regarding the evolution of T_0 in the compounds under applied pressure. For now, we note that the value of the slope in the HO phase (for $x \leq 0.15$) is $\partial T_{HO}/\partial P_{ch} = 1.1$ K GPa^{-1}. This slope was determined from a linear fit to the $T_0(x)$ data that is represented by the symbols in color at the Fe concentrations of $x = 0$ (green circle), $x = 0.025$ (blue diamond), $x = 0.05$ (red diamond), $x = 0.10$ (black triangle) and $x = 0.15$ (cyan square).

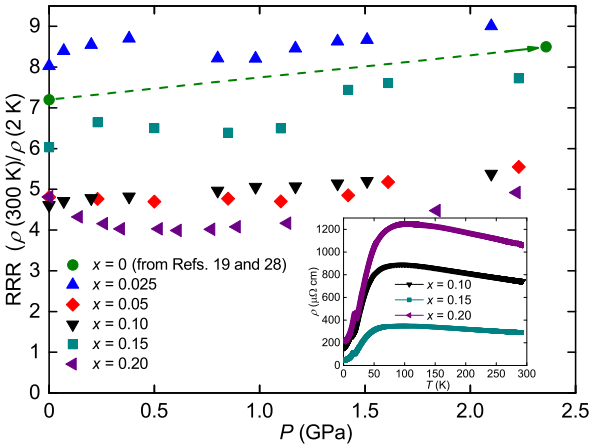

FIG. 2. (Color online) A plot of the residual resistivity ratio (RRR = ρ(300 K)/ρ(2 K)) as a function of pressure, P, for single crystal samples of $URu_{2-x}Fe_xSi_2$ at $x = 0$, 0.025, 0.05, 0.10, 0.15, and 0.20. The two green data points for the $x = 0$ sample at $P = 0$ and 2.4 GPa connected by the dashed green arrow are taken from Refs. 19 and 28. Inset: A plot of the "unshifted" ρ vs. T curves at ambient pressure for the $URu_{2-x}Fe_xSi_2$ (x = 0.10, 0.15, and 0.20) compounds, which displays the drop in the nominal electrical resistivity for the $x = 0.15$ compound relative to the neighboring concentrations of $x = 0.10$ and 0.20.

In this study, we are primarily concerned with the results obtained from the measurements of $\rho(T)$ performed under pressure for the five compounds $URu_{2-x}Fe_xSi_2$ with x = 0.025, 0.05, 0.1, 0.15, and 0.2. However, it should be mentioned that in a related study of the $URu_{2-x}Fe_xSi_2$ system as reported in Ref. 27, bulk property measurements, which included measurements of $\rho(T)$ of single crystals of $URu_{2-x}Fe_xSi_2$ for $x \leq 0.7$, yielded a critical concentration of $x_c^* \approx 0.10$ at the HO → LMAFM transition and a "kink" in the T_0 vs. x phase diagram very similar to the T_0 vs. x phase diagram displayed in Fig. 1. However, in that study, the x dependence of the transition temperature T_{HO} (represented by the solid blue line in the HO phase as shown in Fig. 1) for small increases in the Fe concentration up to $x \approx 0.10$ is somewhat smaller than the positive slope reported herein for the $T_0(x)$ data which are represented by the symbols in color at the Fe concentrations of $x = 0$ (green circle), $x = 0.025$ (blue diamond), $x = 0.05$ (red diamond), $x = 0.10$ (black triangle) and $x = 0.15$ (cyan square). The discrepancy in the x dependence of T_{HO} at low concentrations of Fe between these two studies is largely due to the difference between the initial values of $T_{HO} = 16.5$ K and 17.3 K reported for the parent compound URu_2Si_2 ($x = 0$). While the value of $T_{HO} = 17.3$ K for the ($x = 0$) single crystal was obtained directly from measurements of $\rho(T)$ in Ref. 27, the value of $T_{HO} = 16.5$ K for the ($x = 0$) single crystal was determined from measurements of $\rho(T)$ as reported in Ref. 19.

Since we did not perform measurements of $\rho(T)$ on the parent compound URu_2Si_2 ($x = 0$) under pressure,

the value of $T_{HO} = 16.5$ K from Ref. 19 was included in the present study in order to provide a reference for the $\rho(T, P)$ measurements on the Fe-substituted single crystals of $URu_{2-x}Fe_xSi_2$ with $x = 0.025$, 0.05, 0.10, 0.15, and 0.20. The details regarding both the synthesis of the single crystal of URu_2Si_2 ($x = 0$) in Ref. 19 as well as the experimental conditions for the measurements of $\rho(T)$ of the URu_2Si_2 ($x = 0$) sample under pressure as reported in Ref. 19 are nearly identical to the method of synthesis and experiments reported herein for the measurements of $\rho(T)$ of the Fe-substituted $URu_{2-x}Fe_xSi_2$ single crystal samples under pressure.

However, the fact that the transition temperature of $T_{HO} = 16.5$ K for the URu_2Si_2 parent compound at ambient pressure from Ref. 19 is low compared to T_{HO} values reported in other works as shown in Table II deserves some comment. The various values for T_{HO} listed in Table II are based on measurements of $\rho(T)$ for samples of the URu_2Si_2 parent compound at ambient pressure. The value of T_{HO} may be defined differently from one report to another; for example, in Refs. 19 and 21, T_{HO} is defined to be at the minimum of the anomaly in the $\rho(T)$ curve (as we have defined it in this manuscript); in Refs. 16 and 27, T_{HO} is defined to be at the "inflection point" of the anomaly in the $\rho(T)$ curve, or equivalently, at the minimum in the temperature derivative, $\mathrm{d}\rho/\mathrm{d}T$, of the $\rho(T)$ curve; in Ref. 22, T_{HO} is defined to be at the maximum in the anomaly in the $\rho(T)$ curve.

The low value of $T_{HO} = 16.5$ K from Ref. 19 as compared to the other values of $T_{HO} = 17.8$ K,[16] 17.5 K,[21] 18.0 K,[22] and 17.7 K,[27] (values which are determined from the minimum in the $\rho(T)$ curve), is likely due to issues related to sample quality as well as to extrinsic experimental issues related to differences in the thermometry that can occur during the measurement of $\rho(T)$. Drawing from the conclusions reached in Ref. 29 regarding those issues related to the quality of single crystal samples of URu_2Si_2, it appears that "small" discrepancies in the value of T_{HO} on the order of ~ 0.5 K may result from differences in the residual resistivity ratio (RRR = $\rho(300\text{ K})/\rho(2\text{ K})$) that can occur from one sample to another. While high quality samples with larger values of RRR ~ 100 tend to yield values of $T_{HO} \sim 17.8$ K (defined at the minimum in the $\rho(T)$ curve), samples with smaller values of RRR ~ 10 tend to yield values of $T_{HO} \sim 17.3$ K.[29] Values of RRR that are listed in Table II indicate that the lowest value of RRR = 7.2 corresponds to the lowest value of the $T_{HO} = 16.5$ K,[19] while the largest value of RRR = 100 corresponds to the highest value of the $T_{HO} = 18.0$ K.[22]

The RRR values as a function of pressure, P, are displayed in Fig. 2 for both the single crystal samples of the Fe-substituted $URu_{2-x}Fe_xSi_2$ compounds with $x = 0.025$, 0.05, 0.10, 0.15, and 0.20 reported herein as well as the single crystal sample of URu_2Si_2 ($x = 0$) from Ref. 19.[19,28] For each compound, there is a slight overall increase in the RRR value with an increase in pressure, P: for the $x = 0$ compound, there is an increase in the RRR value from 7.2 at 0 GPa to 8.5 at 2.4 GPa; for the $x = 0.025$ compound, there is an increase in the RRR value from 8.0 at 0 GPa to 9.0 at 2.1 GPa; for the $x = 0.05$ compound, there is an increase in the RRR value from 4.8 at 0 GPa to 5.5 at 2.2 GPa; for the $x = 0.10$ compound, there is an increase in the RRR vlaue from 4.6 at 0 GPa to 5.4 at 2.1 GPa; for the $x = 0.15$ compound, there is an increase in the RRR value from 6.0 at 0 GPa to 7.7 at 2.2 GPa; and for the $x = 0.20$ compound, there is an increase in the RRR value from 4.8 at 0 GPa to 4.9 at 2.2 GPa. We briefly note that there is a large amount of anisotropy observed in the room temperature electrical resistivity for single crystals of the URu_2Si_2 ($x = 0$) parent compound such that $\rho(300\text{ K})$ is roughly two times larger for a measurement of $\rho(T)$ parallel to the a-axis (or basal plane) when compared to a measurement with the current parallel to the c-axis.[30] Hence, the RRR value is sensitive to the orientation of the crystal during the measurement of $\rho(T)$. The RRR values as a function of pressure that are reported in Ref. 28 (which are based on the measurements of $\rho(T)$ for the URu_2Si_2 ($x = 0$) sample from Ref. 19) were determined from measurements of $\rho(T)$ with the current parallel to the a-axis. The quality and orientation of the URu_2Si_2 ($x = 0$) sample from Ref. 19 were determined from Laue X-ray diffraction patterns.

As displayed in Fig. 2, there is also an overall reduction in the RRR value with increasing Fe concentration from $x = 0.025$ to 0.20. However, there is a jump in the RRR value at $x = 0.15$ which is due to the drop in the overall nominal value of the electrical resistivity, $\rho(T)$, for the sample with $x = 0.15$ relative to samples with neighboring concentrations of $x = 0.10$ and 0.20 as dispayed in the inset of Fig. 2. Sudden shifts in the nominal values of the electrical resistivity, $\rho(T)$, may occur during measurements of $\rho(T)$ in a hydrostatic piston-cylinder cell that can affect the electrical contacts between the platinum wire leads that are affixed with silver epoxy to the gold-sputtered samples. The unintended and not entirely understood effects on sample contacts in a four-wire electrical resistivity configuration that result from repeated thermal cycling between $T = 300$ K and 1 K while under applied pressure in a quasi-hydrostatic pressure medium (of isoamyl-alcohol and n-pentane) that freezes at $T \approx 100$ K may cause shifts of the nominal value of $\rho(T)$ from one measurement to the next.

Although the RRR = 7.2 and $T_{HO} = 16.5$ K values for the single crystal sample of URu_2Si_2 from Ref. 19 are low, it is important to note that both the critical pressure, $P_c = 1.5$ GPa, and the pressure dependence in the HO phase, $\partial T_{HO}/\partial P = 1.0$ K GPa^{-1}, as determined from measurements of $\rho(T)$ for the URu_2Si_2 ($x = 0$) sample under pressure in Ref. 19 are consistent with other reports[14–18,20,21] (as shown in Table I). The importance of this point will be addressed below when discussing the additive behavior of chemical pressure, P_{ch}, and applied critical pressure, P_c, such that $P_{ch}(x_c) + P_c \approx 1.5$ GPa for the $URu_{2-x}Fe_xSi_2$ system.

TABLE II. Values of the PM→HO phase transition temperature (T_{HO}) and the residual resistivtiy ratio (RRR) at ambient pressure along with the pressure dependence ($\partial T_{HO}/\partial P$) in the HO phase (if applicable), for samples of the URu_2Si_2 ($x = 0$) parent compound as reported in various works.

Year	Reference	RRR	Crystal	T_{HO} (K)	$\partial T_{HO}/\partial P$ (K GPa^{-1})
1987	McElfresh[16]	37.5	polycrystal	17.4† (17.8*)	1.3 ± 0.1
2007	Jeffries[19]	7.2	single crystal	16.5*	1.0 ± 0.1
2010	Butch[21]	22.5	single crystal	17.5*	1.3 ± 0.1
2011	Kanchanavatee[22]	100	polycrystal	17.5‡ (18.0*)	–
2015	Ran[27]	11.9	single crystal	17.3† (17.7*)	–

* T_{HO} defined at minimum in $\rho(T)$
† T_{HO} defined at inflection point in $\rho(T)$ or at minimum in dρ/dT
‡ T_{HO} defined at maximum in $\rho(T)$

Enhancement of T_0 with pressure

Measurements of electrical resistivity $\rho(T)$ were performed under pressure for each of the compounds $URu_{2-x}Fe_xSi_2$ (x = 0.025, 0.05, 0.10, 0.15, and 0.20). The temperature dependence of $\rho(T)$ at various pressures up to $P \sim 2.2$ GPa in the region near T_0 for the $URu_{2-x}Fe_xSi_2$ ($x = 0.025$ and 0.20) compounds is shown in Fig. 3 (a) and (b), respectively. In the interest of space and to avoid redundancy, data for only two ($x = 0.025$ and 0.20) of the five (x = 0.025, 0.05, 0.10, 0.15, and 0.20) compounds investigated in this report are shown in Fig. 3. The compound with $x = 0.025$, which has the smallest Fe concentration studied, is an example of a $URu_{2-x}Fe_xSi_2$ compound in the HO phase (for $T \leq T_0$) at ambient pressure that undergoes a first-order phase transition to the LMAFM phase as pressure is increased; the compound with $x = 0.20$, which is the largest Fe concentration in this study, represents an example of a $URu_{2-x}Fe_xSi_2$ compound that is already in the LMAFM phase (for $T \leq T_0$) at ambient pressure and remains in that phase as pressure is increased up to the maximum pressure reached in this experiment at $P \sim 2.2$ GPa.

The curves for $\rho(T)$ in both Fig. 3 (a) and (b) have been shifted vertically in order to better illustrate the behavior of the HO/LMAFM transition temperature T_0 as pressure is increased. The enhancement of T_0 can be seen in the shift of the feature in $\rho(T)$ to higher values of temperature as pressure is increased. Electrical resistivity (ρ vs. T) curves for the compounds with Fe concentrations of x = 0.05, 0.10, and 0.15 are not shown but exhibit similar behavior under applied pressure. Measurements of $\rho(T)$ under applied pressure for the two $URu_{2-x}Fe_xSi_2$ (x = 0.05, 0.15) compounds were also performed upon decreasing the pressure in the cell. The pressure was released by unloading the cell stepwise from ∼2.1 GPa to 0 GPa so that additional measurements of $\rho(T)$ could be performed for the purpose of confirming the reversibility of certain portions of the T_0 vs. P phase boundary. We briefly comment here that the results obtained for the evolution of T_0 with increasing pressure were completely

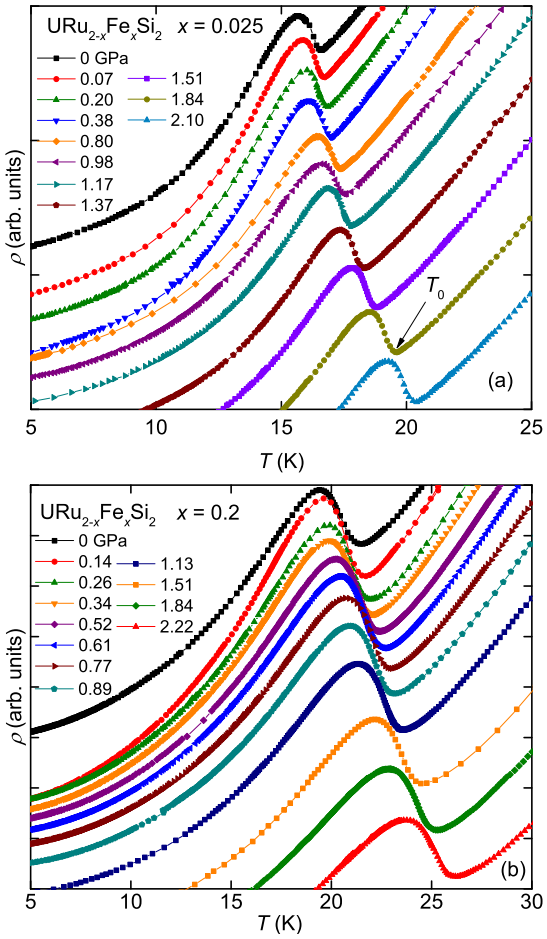

FIG. 3. (Color online) Temperature dependence of electrical resistivity $\rho(T)$ near the HO/LMAFM transition temperature T_0 at various pressures for $URu_{2-x}Fe_xSi_2$ (a) x=0.025 and (b) x=0.2. The $\rho(T)$ curves have been shifted vertically for clarity in illustrating the evolution of the resistivity feature near T_0. (Electrical resistivity curves for the other Fe concentrations, x = 0.05, 0.10, 0.15, are not shown but exhibit similar behavior). The transition temperature T_0 is defined as the temperature at which there is a minimum in $\rho(T)$ as indicated by the black arrow in the upper panel.

reversible upon the release of pressure which can be seen in the $T_0(P)$ data (open symbols) for the x = 0, 0.05, and 0.15 compounds in the T_0 vs. P phase boundary displayed in Fig. 4.

The suppression of the critical pressure P_c with increasing Fe substitution

A composite plot of the T_0 vs. P phase boundaries for various values of x is displayed in Fig. 4. The T_0 vs. P phase boundaries were constructed from features in the $\rho(T)$ curves for the $URu_{2-x}Fe_xSi_2$ (x = 0, 0.025, 0.05, 0.10, 0.15, and 0.20) compounds under pressure, as illustrated in Fig. 3. (The green data points corresponding to the URu_2Si_2 ($x = 0$) compound were taken from

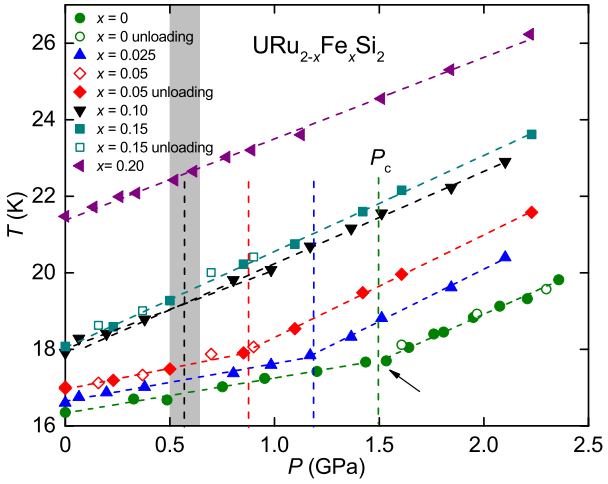

FIG. 4. (Color online) The T_0 vs. P phase diagram for $URu_{2-x}Fe_xSi_2$ (x = 0, 0.025, 0.05, 0.10, 0.15, 0.20). The open symbols for the x = 0, 0.05 and 0.15 data represent data taken upon releasing the pressure. The sloped dashed lines are linear fits to the data. The vertical dashed lines indicate the values of the critical pressure P_c = 1.5, 1.17, 0.85, and 0.57 GPa for x = 0, 0.025, 0.05, and 0.10, respectively. The dashed line for the critical pressure P_c = 0 GPa for x = 0.15 has been omitted. The gray rectangle represents the error in determining the critical pressure, P_c = 0.57, for the x = 0.1 compound. The value of P_c is defined as the pressure at the discontinuity in the dT_0/dP curve as indicated, for example, by the black arrow pointing to the kink in the green data. (The green data points shown for x = 0 were taken from Ref. 19.)

a previous study of URu_2Si_2 under pressure by Jeffries *et al.* in Ref. 19.) The most striking aspect of the T_0 vs. P phase boundaries is the "shift" of the "kink" in the $T_0(P)$ data to lower values of pressure, P, in those $URu_{2-x}Fe_xSi_2$ compounds with higher concentrations of Fe, x. The "kink" in the $T_0(P)$ data signifies the first-order phase transition from the HO phase to the LMAFM phase occurring in the $URu_{2-x}Fe_xSi_2$ compounds with x = 0, 0.025, 0.05, and 0.10. The HO $\rightarrow$ LMAFM phase transition occurs at a critical pressure, P_c, which is defined as the pressure at the location of the discontinuity in the slope, $\partial T_0/\partial P$, i.e., at the "kink" in the $T_0(P)$ data.

We identify the "kink" in the T_0 vs. P phase boundary as the location of a tricritical point at which point the phase boundary between the HO and LMAFM phases (for $T \leq T_0$) joins with the $T_{HO}(P)$ phase boundary between the PM and HO phases and the $T_N(P)$ phase boundary between the PM phase and high pressure LMAFM phase. In this report, we were not able to witness any additional features in the electrical resistivity (below T_{HO}) that would allow for the determination of the HO $\rightarrow$ LMAFM phase boundary.

According to theoretical models,[31,32] it is possible that there may exist a critical end point on the HO $\rightarrow$ LMAFM phase boundary, rather than a tricritical point, if the two ordered phases HO and LMAFM (below T_0) exhibit the same antiferromagnetic symmetry. However, in such a case, the $T_0(P)$ phase boundary between the PM and HO/LMAFM phases would be smooth and absent of a "kink".[31] Recently, neutron scattering experiments reveal that the magnetic and lattice excitations below T_{HO} in the HO phase do not share the broken symmetries observed in the PM $\rightarrow$ LMAFM phase transition at T_N.[33] To the contrary, the excitations in the HO phase appear to reflect the symmetry observed in the PM phase above T_{HO}. We suggest that the suppression of the "kink" with increasing x in $URu_{2-x}Fe_xSi_2$ as observed in the $T_0(P)$ boundary provides additional evidence for the existence of a true tricritical point in the T_0 vs. P phase diagram in which the ordering in the HO phase exhibits a different symmetry than the ordering in the LMAFM phase.[20,31]

From the composite plot of the T_0 vs. P phase boundaries for various values of x shown in Fig. 4, it is clear that there is a complete suppression of the HO phase in favor of the LMAFM phase with increasing Fe concentration, x, such that the critical pressure decreases from P_c = 1.5 GPa at x = 0 to P_c = 0 GPa at x = 0.15. The shift of this tricritical point to lower critical pressure, P_c, in compounds with higher concentrations of Fe, x, is perhaps the defining and most interesting result of this report and suggests a simple additive relation between chemical pressure, P_{ch}, and applied pressure, P, as tuning parameters for investigating the ordered phases in the $URu_{2-x}Fe_xSi_2$ system.

Referring back to the T_0 vs. x phase boundary shown in Fig. 1, it is apparent that the $URu_{2-x}Fe_xSi_2$ compounds, for which $x \geq 0.15$, have already entered the LMAFM phase; in particular, for the $URu_{2-x}Fe_xSi_2$ compound with x = 0.15, the value of the critical pressure is P_c = 0 GPa. Hence, there are no observable kinks in the $T_0(P)$ data shown in Fig. 4 for the $URu_{2-x}Fe_xSi_2$ compounds with x = 0.15 and 0.20. However, there are clear discontinuities in the slope $\partial T_0/\partial P$ for $URu_{2-x}Fe_xSi_2$ compounds with x = 0, 0.025, and 0.05 which occur at values of P_c = 1.5, 1.17, and 0.85 GPa, respectively. At low pressure in the HO phase, the rate of change in T_{HO} with P is $\partial T_{HO}/\partial P \sim 1$ K GPa^{-1} (see Table III below), which is in good agreement with the variation predicted from thermal expansion and specific heat measurements via the Ehrenfest relation.[20,27,34] Note that the pressure coefficient, $\partial T_{HO}/\partial P \sim 1$ K GPa^{-1}, is remarkably consistent with the calculated chemical pressure coefficient, $\partial T_{HO}/\partial P_{ch}$ = 1.1 K GPa^{-1}, which further suggests the similarity between these two types of experimental tuning, x and P.

The discontinuity in $\partial T_0/\partial P$ for the $URu_{2-x}Fe_xSi_2$ compound with x = 0.10 is more difficult to identify and requires some comment. First, there is a smaller difference between the slope $\partial T_{HO}/\partial P$ = 2.06 K GPa^{-1} in the HO phase when compared to the slope $\partial T_N/\partial P$ = 2.42 K GPa^{-1} in the LMAFM phase; one explanation for the elevated value of $\partial T_{HO}/\partial P$ for the $URu_{2-x}Fe_xSi_2$ (x = 0.10) compound is that, below T_{HO}, the sample may consist of a mixture of the HO and LMAFM phases. ^{29}Si NMR,[15] ac susceptibility, and elastic neu-

tron scattering experiments[12] performed on the parent compound URu_2Si_2 under pressure revealed a phase separated spatial inhomogeneity in which the HO phase was populated with regions of LMAFM phase. Elastic neutron scattering measurements performed on single crystals of $URu_{2-x}Fe_xSi_2$ prepared in our lab reveal an increase in the U ordered moment with increasing x in the HO phase, consistent with a scenario in which regions of the LMAFM phase coexist with the HO phase.[23] More recently, muon spin rotation (μSR) measurements on samples of $URu_{2-x}Fe_xSi_2$ prepared in another laboratory demonstrated that the HO phase contains phase separated regions of the LMAFM phase in $URu_{2-x}Fe_xSi_2$ compounds with low levels of Fe concentrations.[35] Second, there is an absence of data in the region where P_c is likely to occur. Hence, $P_c \approx 0.57$ GPa was determined from the intersection of the line of fit to the $T_0(P)$ data in the HO phase (the first four black triangles as shown in Fig. 4) with the line of fit to the $T_0(P)$ data in the LMAFM phase (the remaining seven black triangles as shown in Fig. 4). For ease of comparison, the values of P_c and $\partial T_0/\partial P$ for the $URu_{2-x}Fe_xSi_2$ compounds (x = 0.025, 0.05, 0.10, 0.15, and 0.20) are presented in Table III. Note that the slope ($\partial T_N/\partial P$) in the LMAFM phase is approximately 2.5 times larger than the slope ($\partial T_0/\partial P$) in the HO phase (with the exception of the $URu_{2-x}Fe_xSi_2$ compound with $x = 0.10$).

It is apparent from the slope ($\partial T_0/\partial P$) in the HO and LMAFM phases, that the $URu_{2-x}Fe_xSi_2$ ($x = 0.10$) compound is not fully expressed in the LMAFM phase at ambient pressure. Hence, of the five compounds $URu_{2-x}Fe_xSi_2$ (x = 0, 0.025, 0.05, 0.10, 0.15, and 0.20) that were measured in this study, we determined that $x = 0.15$ is the smallest concentration of Fe in which the $URu_{2-x}Fe_xSi_2$ system is completely in the LMAFM phase, at ambient pressure. The measured value of x_c^* = 0.15 for the critical concentration of Fe is close to the estimated value of x_c^* that was determined from the location of the "kink" in the the T_0 vs. x phase boundary shown in Fig. 1. Further analysis in the last section of this paper shows that $x = 0.15$ is a reasonable determination of the ambient pressure critical concentration of Fe, x_c^*.

TABLE III. Values of the applied critical pressure P_c (for various levels of Fe concentration, x, in the $URu_{2-x}Fe_xSi_2$ system) at the HO $\rightarrow$ LMAFM phase transition along with the pressure dependence ($\partial T_0/\partial P$) in the HO and LMAFM phases.

x	P_c (GPa)	$\partial T_0/\partial P$ (K GPa^{-1})	
		HO phase	LMAFM phase
0 (from Ref. 19)	1.50	1.0 ± 0.1	2.5 ± 0.1
0.025	1.17	1.0 ± 0.1	2.7 ± 0.1
0.05	0.85	1.1 ± 0.1	2.7 ± 0.1
0.10	0.57	2.1 ± 0.1	2.4 ± 0.1
0.15	0.00	–	2.5 ± 0.1
0.20	–	–	2.1 ± 0.1

Pressure dependence of the energy gap Δ

The first bulk property measurements of the specific heat and electrical resistivity for the parent compound URu_2Si_2 ($x = 0$) at ambient pressure suggest that the second-order mean-field-like transition from the paramagnetic (PM) phase to the HO/LMAFM phase results in the opening of a charge gap (Δ) over a portion of the Fermi surface.[1,2,30] Originally, the gapped portion of the Fermi surface for URu_2Si_2 at ambient pressure had been attributed to the formation of a static charge- or spin-density wave (CDW or SDW) below T_0 ~17.5 K while the remaining non-gapped portion of the Fermi surface was thought to be available to superconducting electron states with T_c ~1.5 K.[2,30] In this scenario, the coexistence of superconductivity and HO could be thought of as ordered phases that compete for Fermi surface fraction.[2,19,36] It is now known that the superconductivity is suppressed with chemical substitution x or applied pressure P, and is eventually destroyed during the first-order phase transition from the HO phase to the LMAFM phase.[2,16,37] Additional investigations of the parent compound URu_2Si_2 (x = 0) employing various experimental probes such as infrared spectroscopy,[38] Hall effect,[39–41] quantum oscillation measurements,[42] angle-resolved photoemission spectroscopy (ARPES),[43,44] optical conductivity,[38,45,46] and scanning tunneling microscopy (STM),[47,48] confirm a reorganization of the electronic structure below T_0 which results in a partial gapping of the Fermi surface.

Surprisingly, experiments under pressure, including de Haas-van Alphen (dHvA),[20,49] Shubnikov-de Haas (SdH),[50] and inelastic neutron scattering experiments,[51] reveal that there is no significant change in the gapped structure of the Fermi surface as the URu_2Si_2 compound undergoes a first-order transition from the HO phase to the LMAFM phase. The electronic reconstruction and partial gapping of the Fermi surface for $T < T_{HO}$ has become one of the more salient features of the HO phase. Although there is still no consensus on a physical explanation for the gapping of the Fermi surface below T_{HO}, a significant amount of experimental work has provided detailed information regarding the electronic structure above and below T_0 in URu_2Si_2.

The formation of a similar energy gap (Δ) over the Fermi surface in the Fe-substituted compounds $URu_{2-x}(Fe)_xSi_2$ is evident from recent measurements of electrical resistivity $\rho(T)$, specific heat $C(T)$,[22,23,52] and optical conductivity[24] experiments. Here, we report on values for Δ at the Fermi surface in the HO/LMAFM phase as a function of pressure for the various Fe-substituted compounds $URu_{2-x}Fe_xSi_2$ (x = 0.025, 0.05, 0.10, 0.15, and 0.20). The values of Δ were extracted from fits of the $\rho(T)$ data in the temperature region $T < T_0$ to the expression for electrical resistivity, $\rho(T)$:[25]

$$\rho(T) = \rho_0 + AT^2 + B\Delta^2\sqrt{\frac{T}{\Delta}} \times \left[1 + \frac{2}{3}\left(\frac{T}{\Delta}\right) + \frac{2}{15}\left(\frac{T}{\Delta}\right)^2\right] e^{-\frac{\Delta}{T}}. \quad (1)$$

The exponential term in Equation (1) is the dominant contribution to the electrical resistivity $\rho(T)$ in this temperature region ($T < T_0$) and represents the scattering contribution from the gapped spin excitations that are characteristic of antiferromagnetic ordering.[25] Other scattering contributions to $\rho(T)$ in this temperature region include the residual resistivity ρ_0 and the scattering associated with electron-electron interactions that are characteristic of a Fermi liquid, AT^2. We briefly note that earlier reports on measurements of $\rho(T)$ for high purity URu_2Si_2 ($x = 0$) samples with values of RRR $\sim$ 100 suggest that the AT^2 dependence fails to describe the HO phase which is better described by a power law behavior of AT^α, where $\alpha = 1.6$.[29,53] Furthermore, a power law exponent AT^α, where $\alpha < 2$, is typically required to represent the electrical resistivity $\rho(T)$ in the temperature range just above T_c.[20] However, Fermi liquid behavior is assumed to be valid in the low temperature region down to 2 K in this study owing to substantial levels of Fe solutes present in single crystal samples from the $URu_{2-x}Fe_xSi_2$ system with $x = 0.025$, 0.05, 0.10, 0.15, and 0.20 which exhibited low values of RRR < 10 (see Fig. 2). In addition, there was no evidence for the onset of superconductivity in the $\rho(T)$ curves down to 1 K for any of the Fe-substituted $URu_{2-x}Fe_xSi_2$ ($x =$ 0.025, 0.05, 0.10, 0.15, and 0.20) samples measured in this study. Hence, while a $T^{1.6}$ dependence is likely to apply at low temperatures near 2 K for high-purity parent compounds that exhibit superconductivity with a T_c $\sim$ 1.5K or below, we note that a T^2 dependence is applicable down to $T \sim 2$ K for the "dirty" Fe-substituted compounds measured in this study. The assumption of the existence of Fermi liquid behavior below T_0 in our samples of $URu_{2-x}Fe_xSi_2$ ($x = 0.025$, 0.05, 0.10, 0.15, and 0.20) is supported by the recent optical conductivity experiments performed on $URu_{2-x}Fe_xSi_2$ compounds which demonstrated that scattering processes typical of a Fermi liquid were present in both the HO and LMAFM phases.[24]

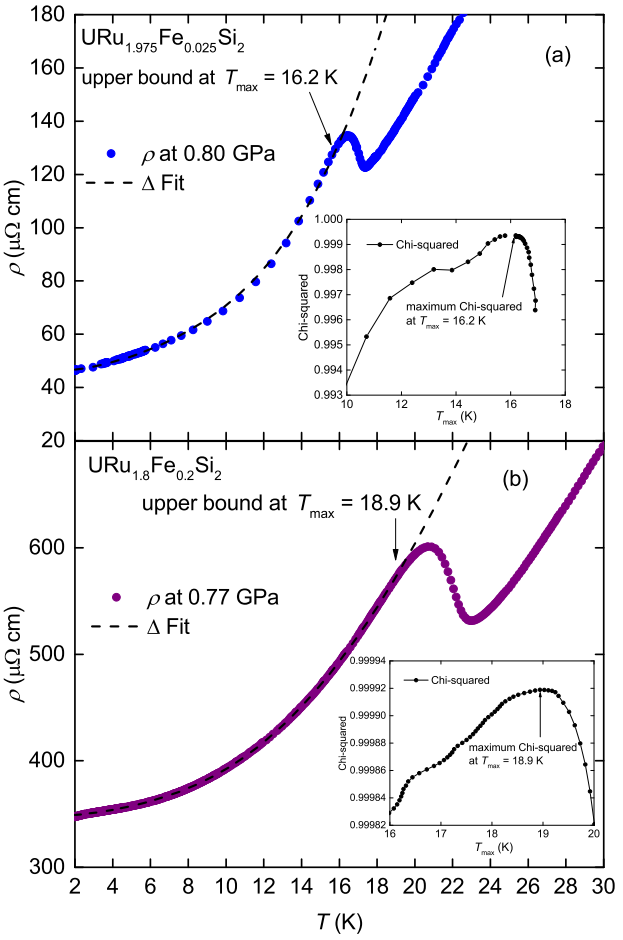

FIG. 5. (Color online) Low temperature electrical resistivity $\rho(T)$ for the (a) $x = 0.025$ compound at 0.8 GPa and (b) $x =$ 0.20 compound at 0.77 GPa plotted along with a theoretical model for the resistivity (see Equation (1) in text), represented by the dashed black curves. The best fit to the $\rho(T)$ data below T_0 was determined by a fitting algorithm as described in the text that allowed for the extraction of the value of the energy gap Δ at various pressures P. Insets: Examples of a plot of Chi-squared vs. T_{max} showing the maximum value of Chi-squared that determined the best fit to the $\rho(T)$ data below T_0.

Examples of curves that were fitted to the $\rho(T)$ data based on Equation (1) for the two $URu_{2-x}Fe_xSi_2$ ($x =$ 0.025 and 0.20) compounds at 0.80 and 0.77 GPa, respectively, are displayed in Fig. 5. The $\rho(T)$ data and the fitted curve (dashed black line) in Fig. 5 (a) correspond to the $URu_{2-x}Fe_xSi_2$ ($x = 0.025$) compound under pressure at $P = 0.80$ GPa which is an example of a $URu_{2-x}Fe_xSi_2$ compound that is in the HO phase for the temperature region of the fit. Similarly, the $\rho(T)$ data and the fitted curve (dashed black line) in Fig. 5 (b) correspond to the $URu_{2-x}Fe_xSi_2$ ($x = 0.2$) compound under pressure at P $= 0.77$ GPa which is an example of a $URu_{2-x}Fe_xSi_2$ compound that is in the LMAFM phase for the temperature region of the fit.

The fit of Equation (1) to the $\rho(T)$ data was performed over the temperature range from $T = 2$ K to T_{max}, where T_{max} represents the upper bound on the temperature range of the $\rho(T)$ data used for the fit. The value of T_{max} was allowed to vary in order to determine the region of data (below T_0) that yielded the best fit. Hence, the best fit of the $\rho(T)$ data to Equation (1) was determined by plotting Chi-squared vs. T_{max} (as displayed in the inset of Fig. 5 (a)). From the Chi-squared vs. T_{max} plot, the determination of T_{max} that yielded the best fit to the $\rho(T)$ data is the value of T_{max} at which Chi-squared is maximized. In the case of the $\rho(T)$ data displayed in Fig. 5 (a), the upper bound in temperature corresponding to the best fit was determined to be $T =$ 16.2 K. In the case of the $\rho(T)$ data displayed in Fig. 5

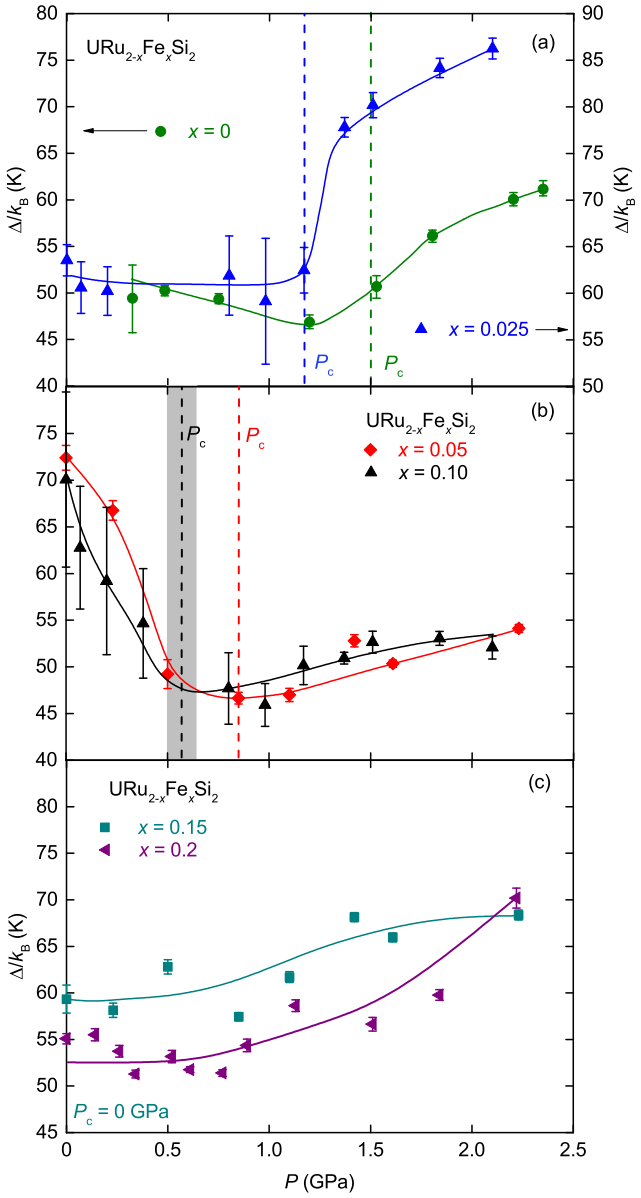

FIG. 6. (Color online) Energy gap Δ vs. pressure P for (a) $x = 0$ and 0.025, (b) $x = 0.05$ and 0.10, and (c) $x = 0.15$ and 0.20. The value of Δ was determined by fitting a theoretical model of electrical resistivity $\rho(T)$ (see Equation (1) in text) to the low temperature electrical resistivity $\rho(T)$ data. The critical pressure P_c and the occurrence of the first-order phase transition from the HO phase to the LMAFM phase are denoted by the dashed vertical lines. The gray rectangle in panel (b) is the error associated in determining the value of P_c for the $x = 0.1$ sample (see text). The values of P_c were determined from the T_0 vs. P phase boundaries shown in Fig. 4. Error bars were determined by the fitting algorithm and the solid curved lines are guides to the eye. (The green data points shown for $x = 0$ were taken from Ref. 19.)

(b), the upper bound in temperature corresponding to the best fit was determined to be $T = 18.9$ K.

The pressure dependence $(\partial\Delta/\partial P)$ of the extracted values of the charge gap (Δ) based on the fits of Equation (1) to the $\rho(T)$ data for the $URu_{2-x}Fe_xSi_2$ (x = 0.025, 0.05, 0.10, 0.15, and 0.20) compounds is displayed in Fig. 6. The $\Delta(P)$ behavior for the URu_2Si_2 ($x = 0$) parent compound from Ref. 19, as displayed in Fig. 6 (a), was determined in a similar fashion; however, a slightly different theoretical model for the electrical resistivity that is based on scattering from gapped ferromagnetic (rather than antiferromagnetic) spin excitations[54,55] was used in the fit to the $\rho(T)$ data in Ref. 19. The differences in the magnitude of Δ extracted from the two different theoretical models of $\rho(T)$ are small and the overall qualitative behavior of the pressure dependence of the gap was shown to be unaffected.[22]

The behavior of $\Delta(P)$ for the six compounds $URu_{2-x}Fe_xSi_2$ ($x = 0$, 0.025, 0.05, 0.10, 0.15, and 0.20) have been grouped and plotted in pairs: ($x = 0$, 0.025), (0.05, 0.10), and (0.15, 0.20) are displayed in Fig. 6 (a), (b), and (c), respectively. The dashed vertical lines in Fig. 6 indicate locations of the critical pressure, P_c, in the $\Delta(P)$ plots and were determined from the T_0 vs. P phase diagram displayed in Fig. 4. For the $URu_{2-x}Fe_xSi_2$ ($x = 0.15$) compound, the vertical dashed line corresponding to a critical pressure at $P_c = 0$ GPa has been omitted. There is a noticeable change in the pressure dependence $(\partial\Delta/\partial P)$ of the gap (Δ) at $P \sim 1.2$, 0.8, and 0.6 GPa for the $URu_{2-x}Fe_xSi_2$ compounds with $x = 0.025$, 0.05, and 0.10, respectively. These values of pressure are remarkably consistent with the critical pressures, $P_c = 1.17$, 0.85, and 0.57 GPa (represented by the vertical dashed lines in Fig. 6). As determined in Ref. 19, there is also a turnaround in the $\Delta(P)$ behavior for the URu_2Si_2 parent compound (green circles in Fig. 6 (a)). The turnaround (or the minimum in $\Delta(P)$) occurs at a pressure of $P \sim 1.3$ GPa, which is slightly lower than the critical pressure, $P_c = 1.5$ GPa. The pressure dependence of the gap $(\partial\Delta/\partial P)$ for the two $URu_{2-x}Fe_xSi_2$ compounds with $x = 0.15$ and 0.20, both of which already exhibit the LMAFM phase at ambient pressure, is displayed in Fig. 6 (c). For these two compounds, there is no non-zero critical pressure, P_c, and hence there is only the monotonic dependence $(\partial\Delta/\partial P > 0$ for $P > 0)$ observed in $\Delta(P)$. The monotonic dependence of $\Delta(P)$ is consistent with the monotonic behavior of $\Delta(P)$ above the critical pressure in the LMAFM phase observed for the other four compounds $URu_{2-x}Fe_xSi_2$ ($x = 0$, 0.025, 0.05, 0.10). (For ease of comparison, there is a correspondence in the color scheme (with regard to Fe concentration, x) between the $\Delta(P)$ curves displayed in Fig. 6 and the $T_0(P)$ data in the plot of the T_0 vs. P phase boundaries displayed in Fig. 4.)

From the plots of $\Delta(P)$ that are displayed in Fig. 6 for the six compounds $URu_{2-x}Fe_xSi_2$ ($x = 0$, 0.025, 0.05, 0.10, 0.15, and 0.20), there is a clear qualitative difference in the $\Delta(P)$ behavior observed in the (low presssure) HO phase, where $\partial\Delta/\partial P < 0$, and the (high pressure) LMAFM phase, where there is a positive pressure coefficient, $\partial\Delta/\partial P > 0$. This behavior seems to be consistent with previous reports on the evolution of the energy gap, Δ, with increases in either x or P. Electrical resistivity measurements performed in an earlier study of single crystals of the parent compound URu_2Si_2 ($x = 0$) under

pressure reveal a monotonic decrease in the Fermi surface gap Δ from $\sim$ 77 to 70 K in the HO phase followed by a jump in Δ to a saturated value of $\sim$ 100 K in the LMAFM phase at $P_x \sim 0.5$ GPa.[56] Similar behavior was observed in the evolution of the energy gap, Δ, as a function of Fe concentration, x. The values for Δ were extracted from a theoretical fit to the specific heat data, $C(T)$, for single crystal samples of $URu_{2-x}Fe_xSi_2$ in which there is a slight suppression of Δ from 93 K down to 80 K in the HO phase for increasing Fe concentration up to $x \sim 0.10$ at which point there is a jump in the value of Δ to $\sim$ 110 K in the LMAFM phase.[23]

It is interesting to note that as the temperature is lowered below T_0, the commensurate $\mathbf{Q_0} = (1,0,0)$ and incommensurate $\mathbf{Q_1} = (1 \pm 0.4,0,0)$ spin excitations in the parent compound URu_2Si_2, exhibit well defined peaks in the energy spectrum which are gapped at energies below $\sim$ 2 meV (or 22 K) and $\sim$ 4.5 meV (or 50 K), respectively.[8,45,57] It has been suggested that below T_0, the two spin excitations at $\mathbf{Q_0}$ and $\mathbf{Q_1}$ are strongly coupled to the charge degree of freedom, suggesting that there is a fundamental relationship between the SDW gaps at $\mathbf{Q_0}$ and $\mathbf{Q_1}$ and the charge (CDW) gap Δ that opens up over the Fermi surface.[45,57,58]

It is now known that the partial gapping of the Fermi surface below T_0 is anisotropic with respect to the a and c axes.[24,45] Furthermore, a comparison of the gapped spin excitations observed in neutron scattering experiments[57] with the energy gaps observed in optical conductivity experiments[24,45] strongly suggests that the anisotropy observed in the charge gap, Δ, over the Fermi surface is such that the a-axis charge gap is linked to the $\mathbf{Q_0}$ spin excitation while the c-axis charge gap is linked to the $\mathbf{Q_1}$ spin excitation.[24,45]

The two different spin excitation gaps, Δ_0 (commensurate) and Δ_1 (incommensurate), are further distinguished in their behavior under applied pressure. While increasing applied pressure has the effect of increasing the energy gap Δ_1, it has the opposite effect of decreasing the energy gap Δ_0.[59] The Δ_0 behavior was confirmed in a later report where the energy gap Δ_0 for the commensurate excitation at $\mathbf{Q_0}$ was observed to monotonically decrease with increasing pressure up until the critical pressure, P_c, at which point the $\mathbf{Q_0}$ excitation completely disappears at the HO $\rightarrow$ LMAFM phase transition.[51] In contrast, the Δ_1 energy gap was observed to increase with pressure in the HO phase below P_c and then survive the first-order HO $\rightarrow$ LMAFM transition at which point Δ_1 jumps discontinuously to a larger value and then remains constant with increasing pressure into the LMAFM phase.[56,60] Here, we simply note the correspondence in the HO phase between the behavior of $\Delta_0(P)$ and the behavior we obtained for $\Delta(P)$ as well as the correspondence in the LMAFM phase between the behavior of $\Delta_1(P)$ and the behavior we observed for $\Delta(P)$.

Our determination of the Fermi surface gap, Δ, which is based on a theoretical model of electrical resistivity fitted to the $\rho(T)$ data from bulk transport measurements under pressure surely cannot capture all of the subtle details that are becoming known regarding the response of the Fermi surface to experimental tuning at temperatures below T_0. Nevertheless, it appears that such a theoretical model of electrical resistivity used in the analysis of bulk measurements of $\rho(T)$ may still capture some of the important features of the charge gap (Δ) that are observed in more direct measurements of the Fermi surface in the HO and LMAFM phases. Namely, the gap analysis performed here seems to capture the differences in the pressure variation, $\partial\Delta/\partial P$, for the HO and LMAFM phases and also finds the magnitude of the charge gap, Δ, to be consistent with previous reports.

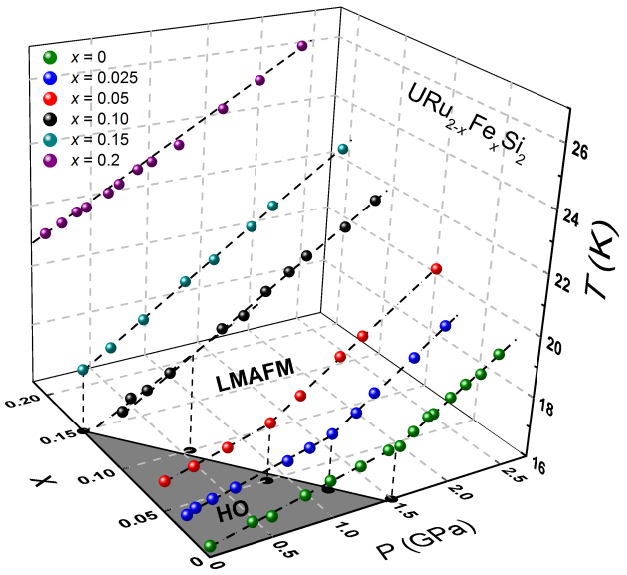

FIG. 7. (Color online) Plot of the T_0 vs. P phase boundaries for various values of x for $URu_{2-x}Fe_xSi_2$ (x = 0, 0.025, 0.05, 0.10, 0.15, and 0.20). The vertical dashed lines drop down to the x-P plane at the respective critical pressures P_c and help determine the boundary between the HO and LMAFM phases in the x-P plane. The HO/LMAFM phase boundary is represented by the solid black line in the x-P plane which is a linear fit of the black circles. At the critical concentration of $x_c^* = 0.15$ and above, the compounds have already entered the LMAFM phase at ambient pressure. (The green data points shown for $x = 0$ are not part of this study and were taken from an earlier study of $URu_{2-x}Fe_xSi_2$ under pressure by Jeffries *et al.* in Ref. 19.)

The simultaneous tuning of URu_2Si_2 with chemical and applied pressure

Perhaps the most interesting aspect of this report is the systematic and predictable manner in which Fe substitution, x, combines with applied pressure, P, to affect the ordered phases and phase transitions observed in URu_2Si_2. The three-dimensional plot of the T_0 vs. P phase boundaries for various values of x displayed in Fig. 7 summarizes the response of the transition temperature, T_0, to the simultaneous tuning of the URu_2Si_2

compound with Fe substitution at $x = 0.025$, 0.05, 0.1, 0.15, and 0.2 while under applied pressure up to $P = 2.2$ GPa. The sloped dashed black lines are linear fits to the six sets of $T_0(P)$ data for the $URu_{2-x}Fe_xSi_2$ compounds at the various Fe concentrations, $x = 0$, 0.025, 0.05, 0.10, 0.15, and 0.20. (The $x = 0$ data were taken from Ref. 19.) There are obvious "kinks" in the $T_0(P)$ data for the $URu_{2-x}Fe_xSi_2$ compounds with $x \leq 0.10$. The "kinks" correspond to the discontinuities in the slope, $\partial T_0/\partial P$, which mark the first-order HO $\rightarrow$ LMAFM phase transition. The slopes, $\partial T_0/\partial P$, of the various $T_0(P)$ curves are presented in Table III along with the values of the critical pressure, P_c, for the respective first-order HO $\rightarrow$ LMAFM phase transitions.

The filled black circles in the x-P plane are the planar projections of the "kinks" (or points of discontinuity in $\partial T_0/\partial P$) that appear in the $T_0(P)$ data (filled colored spheres) of the three dimensional phase diagram. The vertical dashed black lines are drawn to illustrate the planar projections onto the x-P plane. The solid black line in the x-P plane, which represents the phase boundary between the HO phase (gray region) and the LMAFM phase (white region), is a linear fit to the projected points (filled black circles) in the x-P plane. The extrapolation of this linear fit in the x-P plane to the $P = 0$ GPa line indicates that the ambient pressure critical concentration of Fe that forces the transition into the LMAFM phase is $x_c^* = 0.15$. Similarly, the extrapolation of the same linear fit in the x-P plane to the $x = 0$ line indicates that, in the absence of Fe substitution ($x = 0$), the critical pressure that forces the transition into the LMAFM phase is very nearly $P_c = 1.5$ GPa, which is the value of the critical pressure, P_c, that was determined in several reports of other types of measurements of the URu_2Si_2 ($x = 0$) parent compound under pressure (see Table I).

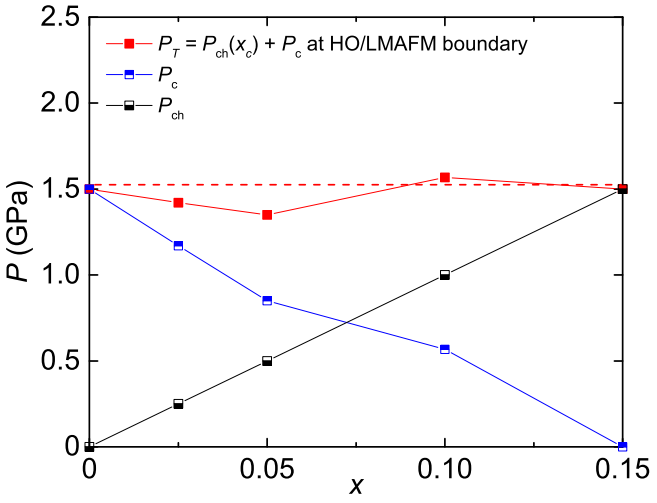

FIG. 8. (Color online) A plot of the chemical pressure P_{ch} (black symbols), critical applied pressure P_c (blue symbols), and the total pressure P_T (red symbols) = $P_{ch}(x_c) + P_c$. The additive behavior of P_{ch} and P_c such that $P_{ch}(x_c) + P_c \approx 1.5$ GPa is consistent with earlier reports on the "kink" in the $T_0(P)$ phase diagram at $P = 1.5$ GPa for the parent compound URu_2Si_2 ($x = 0$).[19]

Hence, the ambient pressure critical concentration of Fe that was determined in this report to be $x_c^* = 0.15$ can be thought to be equivalent to the critical value of applied pressure, $P_c = 1.5$ GPa, that induces the HO $\rightarrow$ LMAFM phase transiton. This allowed us to determine the linear dependence of the chemical pressure, $P_{ch}(x)$, on the Fe concentration x, such that the $P_{ch}(x)$ line, the solid black line shown in Fig. 8, passes through the two points: (P, x) = (0 GPa, 0) and (1.5 GPa, 0.15). We were then able to compare the slope of the $P_{ch}(x)$ line as shown in Fig. 8 with an x to $P_{ch}(x)$ conversion that is based on a bulk modulus β calculation that relates the relative change in the unit cell volume, $\mathrm{d}(V/V_0)$, to the change in pressure, $\mathrm{d}P$: $\beta = 1/\kappa_T = -\mathrm{d}(V/V_0)/\mathrm{d}P$, where V_0 is the initial volume of the unit cell at ambient pressure and κ_T is the isothermal compressibility. From this comparison, we determined the value of the isothermal compressibility for URu_2Si_2: $\kappa_T = 4.5 \times 10^{-3}$ GPa^{-1}. It should be mentioned that a bulk modulus calculation of $P_{ch}(x)$ can vary depending on which value of κ_T is used from the range of values that are reported in the literature. Interestingly, our determination of the value for $\kappa_T = 4.5 \times 10^{-3}$ GPa^{-1} is the mean value of the extreme values of 2×10^{-3} and 7.3×10^{-3} GPa^{-1} reported in the literature.[14,61]

Based on our determination of the $P_{ch}(x)$ line, we note the consistency in which $P_{ch}(x_c) + P_c \approxeq 1.5$ GPa as displayed in Fig. 8. The blue and black half-filled squares represent the chemical pressure, P_{ch}, and critical pressure, P_c, respectively, whereas the filled red squares represent the combined effect of experimental tuning or "total" pressure, $P_T = P_{ch}(x_c) + P_c$, that resulted in a first-order transition from the HO to LMAFM phase. The dashed red line at $P = 1.5$ GPa is for reference and allows for a comparison to the P_T values. Remarkably, for each combination of x and P, the chemical pressure and applied pressure consistently sum to the value of 1.5 GPa to force the HO $\rightarrow$ LMAFM phase transition. The consistency with which the combination of x and P affect the ordered phases in URu_2Si_2 reinforces the idea that the substitution of smaller Fe ions for Ru acts as a "chemical pressure", whereby a reduction in the unit-cell volume affects the compound in a nearly (disregarding disorder) equivalent manner as applying external pressure.

It is clear from the T_0 vs. x phase boundary shown in Fig. 1 that a decrease in the concentration of Fe, which effectively expands the volume of the unit-cell in compounds from the $URu_{2-x}Fe_xSi_2$ series, results in a suppression of T_0. Hence, assuming that "chemical pressure" is the effective mechanism responsible for changes in T_0, an isoelectronic substitution involving a larger ion relative to Ru, such as Os, that results in an expansion of the unit cell volume, should also result in a suppression of T_0. However, experiments on both polycrystalline[52] and sin-

gle crystal[24] samples of $URu_{2-y}Os_ySi_2$ reveal that as the Os concentration, y, is increased in the $URu_{2-y}Os_ySi_2$ series, there is an enhancement, rather than a suppression, in T_0, that is observed in both the HO and LMAFM phases. This behavior is very similar to the evolution of T_0 that is observed with increasing Fe concentration x in the $URu_{2-x}Fe_xSi_2$ series or with increasing pressure, P, for the parent compound URu_2Si_2. Hence, for the Os substituted compounds from the $URu_{2-y}Os_ySi_2$ series, the evolution of T_0 appears to depend on more than "chemical pressure" alone. An investigation involving the experimental tuning of URu_2Si_2 with Os substitution under applied pressure would be interesting in order to answer the question of how a "negative chemical pressure" and an externally applied pressure work together in a system where other mechanisms seem to be at play in affecting T_0 and the HO $\rightarrow$ LMAFM transition. Such an investigation is currently in progress in our laboratory.

IV. CONCLUDING REMARKS

By tuning the parent compound, URu_2Si_2, with an isoelectronic substitution of Fe for Ru, we found that we could bias the material with "chemical pressure" so that a lesser amount of applied external pressure is required to induce the transition to the high pressure LMAFM phase. The results presented here indicate that one can consistently induce the high pressure LMAFM phase in URu_2Si_2 with the appropriate x and P combination that yields $P_{ch}(x) + P_c \cong 1.5$ GPa. The critical values of x and P determined in this report seem to be consistent with previous studies in which the URu_2Si_2 compound was experimentally tuned independently with either x or P.[19,22–24] However, the extra degree of freedom gained in experimentally tuning the URu_2Si_2 compound simultaneously with both x and P offers a number of advantages. Namely, key aspects of the phase diagrams such as the tricritical point (or critical pressure) become dynamic rather than static features that can be tracked with variations in x or P. As an unexpected consequence of the simultaneous tuning of the URu_2Si_2 compound with x and P, we were also able to "measure" the isothermal compressibility, κ_T, for this material and compare its value with others reported in the literature.[14,61]

The suggestion that the response of the URu_2Si_2 compound to "chemical pressure" is nearly equivalent to that of applied pressure presents new opportunities for experiments to be performed on the $URu_{2-x}Fe_xSi_2$ system using STM and ARPES techniques that traditionally cannot be performed under pressure. We further suggest here that the simultaneous tuning of URu_2Si_2 with both Fe substitution and external pressure can serve as a workaround to the current limitations on the amount of pressure that can be applied with the various pressure cells that are used in certain neutron scattering experiments. By experimentally tuning the URu_2Si_2 compound with x, it would be possible to bias the compound with chemical pressure at the outset of the neutron experiment so that larger regions of phase space could be studied in the upper pressure limit where quantum criticality might be explored.

ACKNOWLEDGMENTS

We gratefully acknowledge discussions with P. Riseborough throughout the course of this study. High pressure research at the University of California, San Diego (UCSD) was supported by the National Nuclear Security Administration under the Stewardship Science Academic Alliance Program through the U.S. Department of Energy (DOE) under Grant No. DE-NA0002909. Single crystal growth and characterization at UCSD was supported by the US Department of Energy, Office of Basic Energy Sciences, Division of Materials Sciences and Engineering, under Grant No. DE-FG02-04-ER46105. Low temperature measurements at UCSD were sponsored by the National Science Foundation under Grant No. DMR 1206553.

[1] T. T. M. Palstra, A. A. Menovsky, J. van den Berg, A. J. Dirkmaat, P. H. Kes, G. J. Nieuwenhuys, and J. A. Mydosh, "Superconducting and Magnetic Transitions in the Heavy-Fermion System URu_2Si_2," Phys. Rev. Lett. **55**, 2727–2730 (1985).

[2] M. B. Maple, J. W. Chen, Y. Dalichaouch, T. Kohara, C. Rossel, M. S. Torikachvili, M. W. McElfresh, and J. D. Thompson, "Partially Gapped Fermi Surface in the Heavy-Electron Superconductor URu_2Si_2," Phys. Rev. Lett. **56**, 185–188 (1986).

[3] W. Schlabitz, J. Baumann, B. Pollit, U. Rauchschwalbe, H. M. Mayer, U. Ahlheim, and C. D. Bredl, "Superconductivity and Magnetic Order in a Strongly Interacting Fermi-System: URu_2Si_2," Z. Phys. B - Condensed Matter **62**, 171–177 (1986).

[4] Eric Fawcett, "Spin-density-wave antiferromagnetism in chromium," Rev. Mod. Phys. **60**, 209–283 (1988).

[5] R. A. Fisher, S. Kim, Y. Wu, N. E. Phillips, M. W. McElfresh, M. S. Torikachvili, and M. B. Maple, "Specific heat of URu_2Si_2: Effect of pressure and magnetic field on the magnetic and superconducting transitions," Physica B **163**, 419 – 423 (1990).

[6] J. A. Mydosh and P. M. Oppeneer, "*Colloquium* : Hidden order, superconductivity, and magnetism: The unsolved case of URu_2Si_2," Rev. Mod. Phys. **83**, 1301–1322 (2011).

[7] J. A. Mydosh and P. M. Oppeneer, "Hidden order behaviour in URu_2Si_2 (A critical review of the status of hidden order in 2014)," Philos. Mag. **94**, 3642–3662 (2014).

[8] C. Broholm, J. K. Kjems, W. J. L. Buyers, P. Matthews, T. T. M. Palstra, A. A. Menovsky, and J. A. Mydosh, "Magnetic Excitations and Ordering in the Heavy-Electron Superconductor URu_2Si_2," Phys. Rev. Lett. **58**, 1467–1470 (1987).

[9] E. D. Isaacs, D. B. McWhan, R. N. Kleiman, D. J. Bishop, G. E. Ice, P. Zschack, B. D. Gaulin, T. E. Mason, J. D. Garrett, and W. J. L. Buyers, "X-Ray Magnetic Scattering in Antiferromagnetic URu_2Si_2," Phys. Rev. Lett. **65**, 3185–3188 (1990).

[10] H. Ptasiewicz-Bak, J. Leciejewicz, and A. Zygmunt, "Neutron diffraction study of magnetic ordering in UPd_2Si_2 , UPd_2Ge_2, URh_2Si_2 and URh_2Ge_2," J. Phys. F **11**, 1225 (1981).

[11] L. CheŁmicki, J. Leciejewicz, and A. Zygmunt, "Magnetic properties of UT_2Si_2 and UT_2Ge_2 (T = Co, Ni, Cu) intermetallic systems," J. Phys. Chem. Solids **46**, 529 – 538 (1985).

[12] H. Amitsuka, K. Matsuda, I. Kawasaki, K. Tenya, M. Yokoyama, C. Sekine, N. Tateiwa, T.C. Kobayashi, S. Kawarazaki, and H. Yoshizawa, "Pressure-temperature phase diagram of the heavy-electron superconductor URu_2Si_2," J. of Magn. and Magn. Mater. **310**, 214 – 220 (2007).

[13] P. G. Niklowitz, C. Pfleiderer, T. Keller, M. Vojta, Y.-K. Huang, and J. A. Mydosh, "Parasitic Small-Moment Antiferromagnetism and Nonlinear Coupling of Hidden Order and Antiferromagnetism in URu_2Si_2 Observed by Larmor Diffraction," Phys. Rev. Lett. **104**, 106406 (2010).

[14] H. Amitsuka, M. Sato, N. Metoki, M. Yokoyama, K. Kuwahara, T. Sakakibara, H. Morimoto, S. Kawarazaki, Y. Miyako, and J. A. Mydosh, "Effect of Pressure on Tiny Antiferromagnetic Moment in the Heavy-Electron Compound URu_2Si_2," Phys. Rev. Lett. **83**, 5114–5117 (1999).

[15] K. Matsuda, Y. Kohori, T. Kohara, K. Kuwahara, and H. Amitsuka, "Spatially Inhomogeneous Development of Antiferromagnetism in URu_2Si_2: Evidence from ^{29}Si NMR under Pressure," Phys. Rev. Lett. **87**, 087203 (2001).

[16] M. W. McElfresh, J. D. Thompson, J. O. Willis, M. B. Maple, T. Kohara, and M. S. Torikachvili, "Effect of pressure on competing electronic correlations in the heavy-electron system URu_2Si_2," Phys. Rev. B **35**, 43–47 (1987).

[17] Gaku Motoyama, Takashi Nishioka, and Noriaki K. Sato, "Phase Transition between Hidden and Antiferromagnetic Order in URu_2Si_2," Phys. Rev. Lett. **90**, 166402 (2003).

[18] A. Amato, M. J. Graf, A. de Visser, H. Amitsuka, D. Andreica, and A. Schenck, "Weak-magnetism phenomena in heavy-fermion superconductors: selected μSR studies," J. of Phys.: Condens. Matter **16**, S4403 (2004).

[19] J. R. Jeffries, N. P. Butch, B. T. Yukich, and M. B. Maple, "Competing Ordered Phases in URu_2Si_2: Hydrostatic Pressure and Rhenium Substitution," Phys. Rev. Lett. **99**, 217207 (2007).

[20] E. Hassinger, G. Knebel, K. Izawa, P. Lejay, B. Salce, and J. Flouquet, "Temperature-pressure phase diagram of URu_2Si_2 from resistivity measurements and ac calorimetry: Hidden order and Fermi-surface nesting," Phys. Rev. B **77**, 115117 (2008).

[21] Nicholas P. Butch, Jason R. Jeffries, Songxue Chi, Juscelino Batista Leão, Jeffrey W. Lynn, and M. B. Maple, "Antiferromagnetic critical pressure in URu_2Si_2 under hydrostatic conditions," Phys. Rev. B **82**, 060408 (2010).

[22] N. Kanchanavatee, M. Janoschek, R. E. Baumbach, J. J. Hamlin, D. A. Zocco, K. Huang, and M. B. Maple, "Twofold enhancement of the hidden-order/large-moment antiferromagnetic phase boundary in the $URu_{2-x}Fe_xSi_2$ system," Phys. Rev. B **84**, 245122 (2011).

[23] Pinaki Das, N. Kanchanavatee, J. S. Helton, K. Huang, R. E. Baumbach, E. D. Bauer, B. D. White, V. W. Burnett, M. B. Maple, J. W. Lynn, and M. Janoschek, "Chemical pressure tuning of URu_2Si_2 via isoelectronic substitution of Ru with Fe," Phys. Rev. B **91**, 085122 (2015).

[24] Jesse S. Hall, M. R. Movassagh, M. N. Wilson, G. M. Luke, N. Kanchanavatee, K. Huang, M. Janoschek, M. B. Maple, and T. Timusk, "Electrodynamics of the antiferromagnetic phase in URu_2Si_2," Phys. Rev. B **92**, 195111 (2015).

[25] M. B. Fontes, J. C. Trochez, B. Giordanengo, S. L. Bud'ko, D. R. Sanchez, E. M. Baggio-Saitovitch, and M. A. Continentino, "Electron-magnon interaction in RNiBC (R = Er, Ho, Dy, Tb, and Gd) series of compounds based on magnetoresistance measurements," Phys. Rev. B **60**, 6781–6789 (1999).

[26] T. F. Smith, C. W. Chu, and M. B. Maple, "Superconducting manometers for high pressure measurement at low temperature," Cryogenics **9**, 53 (1969).

[27] S. Ran, C. T. Wolowiec, I. Jeon, N. Pouse, N. Kanchanavatee, K. Huang, D. Martien, T. DaPron, D. Snow, M. Williamsen, S. Spagna, P. S. Riseborough, and M. B. Maple, "Phase diagram and thermal expansion measurements on the system of $URu_{2-x}Fe_xSi_2$," (2016), arXiv:1604.00983v1 [cond-mat.str-el].

[28] J. R. Jeffries, N. P. Butch, B. T. Yukich, and M. B. Maple, "The evolution of the ordered states of single-crystal URu_2Si_2 under pressure," J. of Phys.: Condens. Matter **20**, 095225 (2008).

[29] Tatsuma D. Matsuda, Elena Hassinger, Dai Aoki, Valentin Taufour, Georg Knebel, Naoyuki Tateiwa, Etsuji Yamamoto, Yoshinori Haga, Yoshichika Ōnuki, Zachary Fisk, and Jacques Flouquet, "Details of Sample Dependence and Transport Properties of URu_2Si_2," J. Phys. Soc. Jpn. **80**, 114710 (2011).

[30] T. T. M. Palstra, A. A. Menovsky, and J. A. Mydosh, "Anisotropic electrical resistivity of the magnetic heavy-fermion superconductor URu_2Si_2," Phys. Rev. B **33**, 6527–6530 (1986).

[31] V. P. Mineev and M. E. Zhitomirsky, "Interplay between spin-density wave and induced local moments in URu_2Si_2," Phys. Rev. B **72**, 014432 (2005).

[32] N. Shah, P. Chandra, P. Coleman, and J. A. Mydosh, "Hidden order in URu_2Si_2," Phys. Rev. B **61**, 564–569 (2000).

[33] Nicholas P. Butch, Michael E. Manley, Jason R. Jeffries, Marc Janoschek, Kevin Huang, M. B. Maple, Ayman H. Said, Bogdan M. Leu, and Jeffrey W. Lynn, "Symmetry and correlations underlying hidden order in URu_2Si_2," Phys. Rev. B **91**, 035128 (2015).

[34] A. de Visser, F. E. Kayzel, A. A. Menovsky, J. J. M. Franse, J. van den Berg, and G. J. Nieuwenhuys, "Thermal expansion and specific heat of monocrystalline URu_2Si_2," Phys. Rev. B **34**, 8168–8171 (1986).

[35] M. N. Wilson, T. J. Williams, Y.-P. Cai, A. M. Hallas, T. Medina, T. J. Munsie, S. C. Cheung, B. A. Frandsen, L. Liu, Y. J. Uemura, and G. M. Luke, "Antiferromagnetism and hidden order in isoelectronic doping of URu_2Si_2," Phys. Rev. B **93**, 064402 (2016).

[36] Griff Bilbro and W. L. McMillan, "Theoretical model of superconductivity and the martensitic transformation in $A15$ compounds," Phys. Rev. B **14**, 1887–1892 (1976).

[37] Y. Dalichaouch, M. B. Maple, J. W. Chen, T. Kohara, C. Rossel, M. S. Torikachvili, and A. L. Giorgi, "Effect of transition-metal substitutions on competing electronic transitions in the heavy-electron compound URu_2Si_2," Phys. Rev. B **41**, 1829–1836 (1990).

[38] D. A. Bonn, J. D. Garrett, and T. Timusk, "Far-Infrared Properties of URu_2Si_2," Phys. Rev. Lett. **61**, 1305–1308

(1988).
[39] J. Schoenes, C. Schönenberger, J. J. M. Franse, and A. A. Menovsky, "Hall-effect and resistivity study of the heavy-fermion system URu_2Si_2," Phys. Rev. B **35**, 5375–5378 (1987).
[40] Y. S. Oh, Kee Hoon Kim, P. A. Sharma, N. Harrison, H. Amitsuka, and J. A. Mydosh, "Interplay between Fermi Surface Topology and Ordering in URu_2Si_2 Revealed through Abrupt Hall Coefficient Changes in Strong Magnetic Fields," Phys. Rev. Lett. **98**, 016401 (2007).
[41] Y. Kasahara, T. Iwasawa, H. Shishido, T. Shibauchi, K. Behnia, Y. Haga, T. D. Matsuda, Y. Onuki, M. Sigrist, and Y. Matsuda, "Exotic Superconducting Properties in the Electron-Hole-Compensated Heavy-Fermion "Semimetal" URu_2Si_2," Phys. Rev. Lett. **99**, 116402 (2007).
[42] M. M. Altarawneh, N. Harrison, S. E. Sebastian, L. Balicas, P. H. Tobash, J. D. Thompson, F. Ronning, and E. D. Bauer, "Sequential Spin Polarization of the Fermi Surface Pockets in URu_2Si_2 and Its Implications for the Hidden Order," Phys. Rev. Lett. **106**, 146403 (2011).
[43] Andrés F. Santander-Syro, Markus Klein, Florin L. Boariu, Andreas Nuber, Pascal Lejay, and Friedrich Reinert, "Fermi-surface instability at the 'hidden-order' transition of URu_2Si_2," Nat. Phys. **5**, 637 (2009).
[44] C. Bareille, F. L. Boariu, H. Schwab, P. Lejay, F. Reinert, and A. F. Santander-Syro, "Momentum-resolved hidden-order gap reveals symmetry breaking and origin of entropy loss in URu_2Si_2," Nat. Commun. **5**, 637 (2009).
[45] Jesse S. Hall, Urmas Nagel, Taaniel Uleksin, Toomas Rõõm, Travis Williams, Graeme Luke, and Thomas Timusk, "Observation of multiple-gap structure in hidden order state of URu_2Si_2 from optical conductivity," Phys. Rev. B **86**, 035132 (2012).
[46] R. P. S. M. Lobo, J. Buhot, M. A. Méasson, D. Aoki, G. Lapertot, P. Lejay, and C. C. Homes, "Optical conductivity of URu_2Si_2 in the Kondo liquid and hidden-order phases," Phys. Rev. B **92**, 045129 (2015).
[47] A. R. Schmidt, M. H. Hamidian, P. Wahl, F. Meier, A. V. Balatsky, J. D. Garrett, T. J. Williams, G. M. Luke, and J. C. Davis, "Imaging the Fano lattice to 'hidden order' transition in URu_2Si_2," Nature **465**, 570 (2010).
[48] Pegor Aynajian, Eduardo H. da Silva Neto, Colin V. Parker, Yingkai Huang, Abhay Pasupathy, John Mydosh, and Ali Yazdani, "Visualizing the formation of the Kondo lattice and the hidden order in URu_2Si_2," Proc. Natl. Acad. Sci. **107**, 10383–10388 (2010).
[49] M. Nakashima, H. Ohkuni, Y. Inada, R. Settai, Y. Haga, E. Yamamoto, and Y. Onuki, "The de Haas-van Alphen effect in URu_2Si_2 under pressure," J. of Phys.: Condens. Matter **15**, S2011 (2003).
[50] E. Hassinger, G. Knebel, T. D. Matsuda, D. Aoki, V. Taufour, and J. Flouquet, "Similarity of the Fermi Surface in the Hidden Order State and in the Antiferromagnetic State of URu_2Si_2," Phys. Rev. Lett. **105**, 216409 (2010).
[51] A. Villaume, F. Bourdarot, E. Hassinger, S. Raymond, V. Taufour, D. Aoki, and J. Flouquet, "Signature of hidden order in heavy fermion superconductor URu_2Si_2: Resonance at the wave vector $Q_0 = (1, 0, 0)$," Phys. Rev. B **78**, 012504 (2008).
[52] N. Kanchanavatee, B.D. White, V.W. Burnett, and M.B. Maple, "Enhancement of the hidden order/large moment antiferromagnetic transition temperature in the $URu_{2-x}Os_xSi_2$ system," Philos. Mag. **94**, 3681–3690 (2014).
[53] Nayouki Tateiwa, Tatsuma D. Matsuda, Y Ōnuki, Yoshinori Haga, and Zachary Fisk, "Strong correlation between anomalous quasiparticle scattering and unconventional superconductivity in the hidden-order phase of URu_2Si_2," Phys. Rev. B **85**, 054516 (2012).
[54] Niels Hessel Andersen and Henrik Smith, "Electron-magnon interaction and the electrical resistivity of Tb," Phys. Rev. B **19**, 384–387 (1979).
[55] N. Hessel Andersen, in *Crystalline Electric Field and Structural Effects in f-Electron Systems*, edited by J. E. Crow, R. P. Guertin, and T. W. Mihalisin (Plenum, New York, 1980) p. 373.
[56] Frederic Bourdarot, Elena Hassinger, Stephane Raymond, Dai Aoki, Valentin Taufour, Louis-Pierre Regnault, and Jacques Flouquet, "Precise Study of the Resonance at Q_0=(1,0,0) in URu_2Si_2," J. Phys. Soc. Jpn. **79**, 064719 (2010).
[57] C. R. Wiebe, J. A. Janik, G. J. MacDougall, G. M. Luke, J. D. Garrett, H. D. Zhou, Y.-J. Jo, L. Balicas, Y. Qiu, J. R. D. Copley, Z. Yamani, and W. J. L. Buyers, "Gapped itinerant spin excitations account for missing entropy in the hidden-order state of URu_2Si_2," Nat. Phys **3**, 96 (2007).
[58] C. Broholm, H. Lin, P. T. Matthews, T. E. Mason, W. J. L. Buyers, M. F. Collins, A. A. Menovsky, J. A. Mydosh, and J. K. Kjems, "Magnetic excitations in the heavy-fermion superconductor URu_2Si_2," Phys. Rev. B **43**, 12809–12822 (1991).
[59] F. Bourdarot, A. Bombardi, P. Burlet, M. Enderle, J. Flouquet, P. Lejay, N. Kernavanois, V.P. Mineev, L. Paolasini, M.E. Zhitomirsky, and B. Fåk, "Hidden order in URu_2Si_2," Physica B **359-361**, 986 (2005).
[60] Frederic Bourdarot, Stephane Raymond, and Louis-Pierre Regnault, "Neutron scattering studies on URu_2Si_2," Philos. Mag. **94**, 3702–3722 (2014).
[61] K. Kuwahara, H. Sagayama, K. Iwasa, M. Kohgi, S. Miyazaki, J. Nozaki, J. Nogami, M. Yokoyama, H. Amitsuka, H. Nakao, and Y. Murakami, "High pressure X-ray diffraction study of URu_2Si_2," Acta Phys. Pol. B **34**, 4307 (2003).